Received: 17 February 2021 | Revised: 25 June 2021 | Accepted: 18 July 2021

DOI: 10.1002/jbm.b.34922

RESEARCH ARTICLE

Society For Biomaterials | WILEY

Functionalized polyanhydride nanoparticles for improved treatment of mitochondrial dysfunction

Benjamin W. Schlichtmann[1] | Balaraman Kalyanaraman[2] | Rainie L. Schlichtmann[1] | Matthew G. Panthani[1] | Vellareddy Anantharam[3,4] | Anumantha G. Kanthasamy[3,4] | Surya K. Mallapragada[1,4,5] | Balaji Narasimhan[1,4]

[1]Department of Chemical and Biological Engineering, Iowa State University, Ames, Iowa, USA

[2]Department of Biophysics, Medical College of Wisconsin, Milwaukee, Wisconsin, USA

[3]Department of Biomedical Sciences, Iowa State University, Ames, Iowa, USA

[4]Nanovaccine Institute, Iowa State University, Ames, Iowa, USA

[5]Department of Materials Science and Engineering, Iowa State University, Ames, Iowa, USA

Correspondence
Balaji Narasimhan, Department of Chemical and Biological Engineering, Iowa State University, 5001 ATRB, 2213 Pammel Drive, Ames, IA 50011, USA.
Email: nbalaji@iastate.edu

Funding information
Iowa State Nanovaccine Institute; US Army Medical Research and Materiel Command, Grant/Award Number: W81XWH-11-1-0700

Abstract

Parkinson's disease (PD) is a devastating neurodegenerative disease affecting a large proportion of older adults. Exposure to pesticides like rotenone is a leading cause for PD. To reduce disease progression and prolong life expectancy, it is important to target disease mechanisms that contribute to dopaminergic neuronal atrophy, including mitochondrial dysfunction. Achieving targeted mitochondrial delivery is difficult for many therapeutics by themselves, necessitating higher therapeutic doses that could lead to toxicity. To minimize this adverse effect, targeted nano-carriers such as polyanhydride nanoparticles (NPs) can protect therapeutics from degradation and provide sustained release, enabling fewer administrations and lower therapeutic dose. This work expands upon the use of the polyanhydride NP platform for targeted drug delivery by functionalizing the polymer with a derivative of triphenylphosphonium called (3-carboxypropyl) triphenylphosphonium (CPTP) using a novel method that enables longer CPTP persistence on the NPs. The extent to which neurons internalized both nonfunctionalized and functionalized NPs was tested. Next, the efficacy of these nanoformulations in treating rotenone-induced mitochondrial dysfunction in the same cell line was evaluated using a novel neuroprotective drug, mito-metformin. CPTP functionalization significantly improved NP internalization by neuronal cells. This was correlated with significant protection by CPTP-functionalized, mito-metformin encapsulated NPs against rotenone-induced mitochondrial dysfunction. However, nonfunctionalized, mito-metformin encapsulated NPs and soluble mito-metformin administered at the same dose did not significantly protect cells from rotenone-induced toxicity. These results indicate that the targeted NP platform can provide enhanced dose-sparing and potentially reduce the occurrence of systemic side-effects for PD therapeutics.

KEYWORDS
metformin, Parkinson's disease, polymeric nanoparticles, rotenone, triphenylphosphonium

Abbreviations: AMPK, adenosine monophosphate-activated protein kinase; BBB, blood–brain barrier; CPH, 1,6-bis(*p*-carboxyphenoxy)hexane; CPTP, (3-carboxypropyl)triphenylphosphonium; M:NF-NPs or M:CPTP-NPs, Mito-Met-loaded NF-NPs and CPTP-NPs; NF-NPs and CPTP-NPs, Non- and CPTP-functionalized NPs; NP, nanoparticles; PD, Parkinson's disease; QD:NF-NPs and QD:CPTP-NPs, QD-loaded NF-NPs and CPTP-NPs; RPMI, Roswell Park Memorial Institute medium; SA, sebacic acid; TPP, triphenylphosphonium.

1 | INTRODUCTION

Parkinson's disease (PD) is the world's second most common neurodegenerative disease, with as many as 10 million people living with the disease worldwide and associated direct and indirect costs of PD nearing $25 billion in the United States alone.[1] PD is caused by a combination of environmental and genetic factors, with toxic chemicals like pesticides being a key factor in environmental causes.[2] Currently approved therapeutics used to treat PD only alleviate the motor symptoms to the disease. However, to slow disease progression, it is imperative to develop therapeutics that target the underlying disease mechanisms induced by these factors.[3]

One of the signature mechanisms in PD is mitochondrial dysfunction.[4] Inactivation of complex I of the mitochondrial transport chain is primary contributor to this pathological characteristic.[4] Some challenge models for assessment of PD-associated toxicity therefore use toxic chemicals, often pesticides, to induce mitochondrial dysfunction. One such chemical is rotenone, which is highly toxic to most cells, and acts by impeding complex I of the mitochondrial respiratory chain, leading to subsequent oxidative stress in the brain.[4,5] This model has been shown to induce mitochondrial dysfunction and oxidative stress both in vitro,[5] and in vivo, as previous work with a mouse model has shown that intragastric administration of rotenone can lead to PD-associated degeneration.[6]

Protein kinase C delta activation plays a role in dopaminergic neuronal atrophy by contributing to oxidative stress and mitochondrial dysfunction.[7] In the process, adenosine monophosphate-activated protein kinase (AMPK), an important protein in maintaining cellular metabolism, is downregulated.[8] Furthermore, inhibition of AMPK is closely associated with dopaminergic cell death.[9] Recently, the Type 2 diabetic drug metformin has been proposed as a therapeutic for PD because it activates AMPK.[10] and counteracts the dopaminergic-specific neurodegenerative effects of 3,4-methylenedioxymethamphetamine.[10] Activation of AMPK by metformin stems from the mitochondrial respiration-inhibiting properties of this drug.[11] Therefore, for use of drugs like metformin in treating mitochondrial dysfunction, efficient mitochondrial targeting is essential.

To enhance mitochondrial targeting, the cationic and lipophilic cation, triphenylphosphonium (TPP), has been conjugated to metformin (i.e., Mito-Met).[12] At lower concentrations, Mito-Met is not toxic and induces cell-cycle arrest.[11] Mito-Met induces mitophagy through the activation of AMPK.[13] Neuronal cells conserve energy via this mechanism.[14] A 10-carbon chain derivative of Mito-Met has shown protection against the mitochondria-targeted toxins rotenone and 1-methyl-4-phenylpyridinium in dopaminergic cells.[12] TPP has also been conjugated to apocynin, that is, Mito-Apo to more effectively combat oxidative stress.[15,16] These studies indicate that Mito-Apo and Mito-Met elicit other neuroprotective mechanisms as well. A key difference between such mitochondrially-targeted drugs and rotenone is that rotenone does not induce the energy sensing signaling mechanism provided by Mito-Apo or Mito-Met. Therefore, the neuroprotective mechanisms of metformin outweigh the neurotoxic effects of rotenone, providing a basis for the use of a rotenone-based challenge model for direct assessment of the neuroprotective mechanisms of Mito-Met.[4,5]

However, therapeutics are still systemically administered in a bolus dose, which means frequent administrations are required for treating dopaminergic degeneration. Therefore, the therapeutic frequency and dose can be further minimized using nanoparticles (NPs). NPs can encapsulate therapeutics, protect them from degradation, and release them upon reaching the targeted area to optimize therapeutic efficacy.[17-19] Biodegradable polyanhydride NPs represent a platform with capabilities for sustained release of therapeutics.[20-27] Polyanhydrides are biocompatible and safe,[28-31] they are components of U.S. FDA-approved formulations as exemplified by the Gliadel® wafer,[32] and their hydrophobic nature enables predictable NP-drug release profiles that can be precisely tuned,[30,33-37] compared to less controllable release profiles from the more commonly used and FDA-approved bulk-eroding poly(lactic-co-glycolic acid) (PLGA). These attributes of polyanhydride NPs can further result in dose-sparing effects.[26,38,39]

Polyanhydride chemistries rich in sebacic acid (SA) have recently shown significantly higher levels of cellular internalization by macrophages, primarily by phagocytosis.[40] Our previous work showed that a polyanhydride NP formulation of 20 mol% 1,6-bis (*p*-carboxyphenoxy) hexane (CPH) and 80 mol% SA (i.e., 20:80 CPH:SA) significantly lowered the dose of mito-apocynin required to protect against oxidative stress in dopaminergic cells in vitro.[26] Importantly, this formulation was internalized by monocytes and human brain microvascular endothelial cells (HBMECs), and NP transfer between monocytes and HBMECs was observed in vitro in a blood–brain barrier (BBB) model. This indicates that both cell-mediated and adsorptive-mediated transcytosis mechanisms may be exhibited by SA-rich chemistries, which can improve local bioavailability of therapeutics.[41] Therefore, SA-rich NPs may represent a promising nanomedicine carrier for brain delivery.

While TPP has been conjugated to drugs, it has also been conjugated to NPs to improve brain localization and mitochondrial targeting.[42-47] Polyanhydride NPs have been surface functionalized with targeting ligands to improve protection against oxidative stress in vitro,[26] but the surface-eroding nature of polyanhydride NPs typically results in short ligand retention times that may limit the duration of improved targeting in vivo. Therefore, a novel functionalization method was developed in this work that conjugates the copolymer to the molecule (3-carboxypropyl)triphenyl-phosphonium (CPTP), a derivative of TPP, prior to NP synthesis so that CPTP is retained on the NPs for longer periods of time. Overall, the goal of this work was to test the extent by which CPTP functionalization improves the internalization of the associated NPs into neurons, and whether this is correlated with the ability to improve protection provided by nano-formulated Mito-Met against rotenone-induced mitochondrial dysfunction.

2 | MATERIALS AND METHODS

2.1 | Materials

MitoTracker® Red, Sytox™ Green, Hoechst 33258, Roswell Park Memorial Institute medium (RPMI 1640), Dulbecco's Modified Eagle's

Medium, methylene chloride, methanol, pentane and hexanes were purchased from ThermoFisher Scientific (Waltham, MA). Fetal bovine serum, trypsin/ethylene diamine tetra acedic acid, paraformaldehyde, L-glutamine, penicillin, and streptomycin were purchased from Invitrogen (Carlsbad, CA). CPTP bromide was purchased from Sigma Aldrich (St. Louis, MO). 20:80 CPH:SA copolymer, Mito-Met and cadmium selenide core-shell quantum dots (QDs) were synthesized as described previously.[41]

2.2 | Polyanhydride bulk functionalization and purification

Polyanhydrides were functionalized with CPTP using a bulk functionalization process (Figure 1a). Specifically, CPTP was acetylated by stirring 200 mg CPTP in 25 mL acetic anhydride under nitrogen (N_2) for 60 min at 150°C. Excess acetic anhydride was evaporated, and CPTP was added to 1 g of 20:80 CPH:SA copolymer at 0.5 Torr for 30 min at 180°C. The functionalized copolymer was dissolved in 20 mL methylene chloride overnight, precipitated into hexanes at 1:25 methylene chloride: hexanes and vacuum filtered.

The dried, functionalized polymer was suspended in 30 mL methanol, vortexed for 30 s, and centrifuged at 10,000 rpm for 5 min, removing supernatant. Remaining purified polymer was dried under vacuum. Percentage end-group functionalization was quantified by dissolving in deuterated chloroform and analyzing using ^{1}H nuclear magnetic resonance end-group analysis with an MR400 instrument (Varian, Palo Alto, CA). Fourier transform infrared spectroscopy—attenuated total reflectance was used to confirm polymer functionalization using a Nicolet™ iS50 instrument with the Nicolet™ Smart iTX accessory (ThermoFisher Scientific, Waltham, MA).

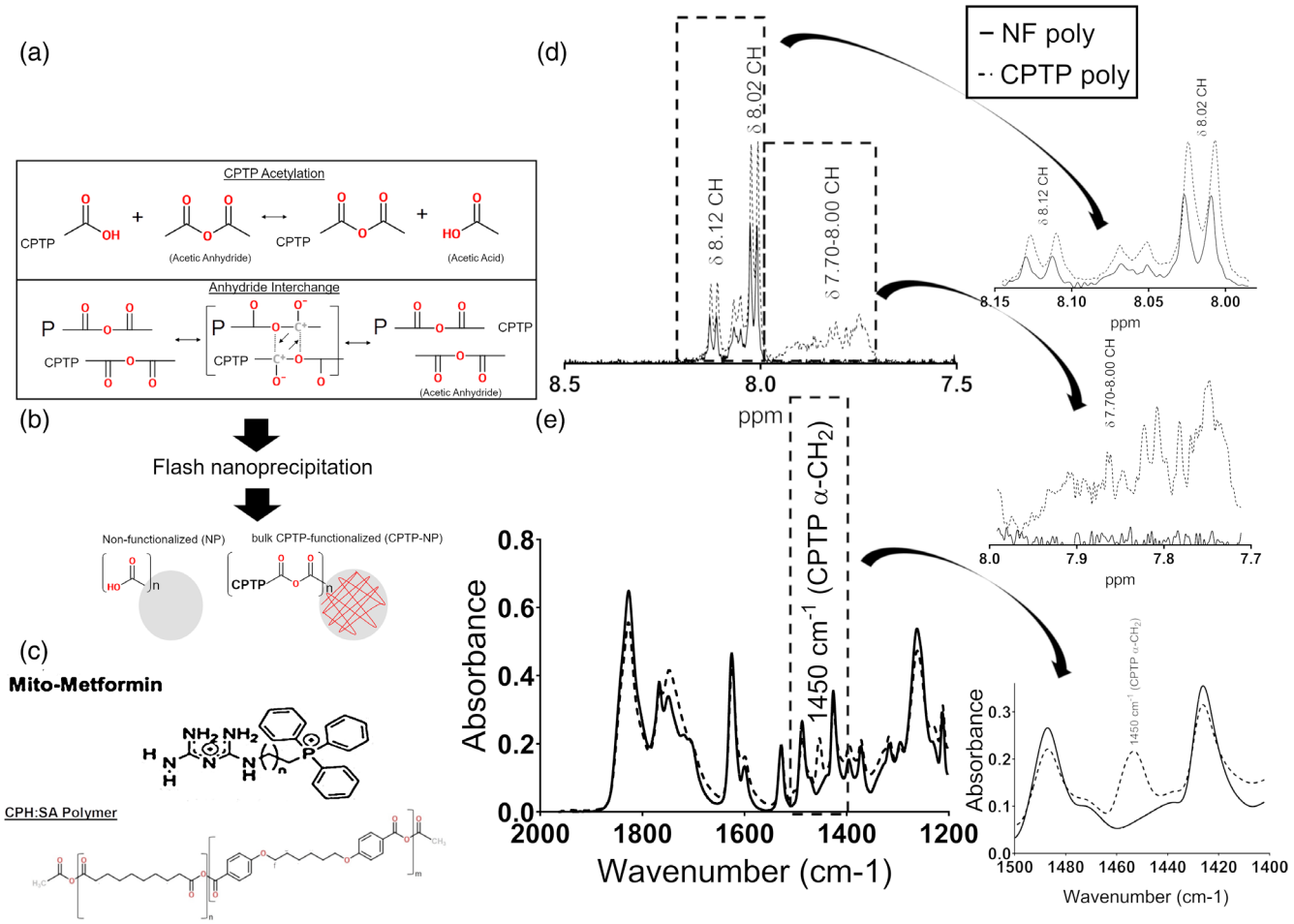

FIGURE 1 (a) Schematic describing the synthesis of functionalized polyanhydrides. The targeting ligand, CPTP, is first acetylated and then reacted with copolymer ("P") at standard polymer synthesis conditions. (b) NPs are synthesized by a flash nanoprecipitation method, resulting in the formation of NPs with either COOH (i.e., nonfunctionalized) or CPTP (i.e., functionalized) end-group moieties. Schematic of Mito-Met structure, encapsulated by NPs for efficacy studies and tested versus soluble dose. Mito-Met C10 ($n = 9$) was used for the study. (d) ^{1}H nuclear magnetic resonance spectra of functionalized, purified polymer showing a CPTP phenyl group CH peak (δ 7.70–8.00, multiplet) alongside polymer CPH phenyl group CH peaks (δ 8.02, doublet; δ 8.12, doublet), and (e) Fourier transform infrared spectroscopy—attenuated total reflectance spectra of functionalized, purified polymer showing a CPTP α-CH_2 bending peak (1450 cm^{-1}). Controls included CPTP only (not shown) and nonfunctionalized polymer only (shown)

2.3 | Nanoparticle synthesis and characterization

QD or Mito-Met (Figure 1c) at 1% (w/w) or 0.2% (w/w), respectively, were encapsulated by NPs using an anti-solvent nano-encapsulation method, described previously (Figure 1b).[41] Briefly, QD or Mito-Met was added to nonfunctionalized 20:80 CPH:SA copolymer dissolved in methylene chloride at 20 mg/mL while sonicating at 30% for 30s and immediately precipitated into pentane (Thermo Fisher Scientific) at room temperature at a 1:250 methylene chloride: pentane ratio. Non- and CPTP-functionalized NPs (NF-NPs and CPTP-NPs, respectively) were made at room temperature and 4°C, respectively. NP morphology and size were determined using a 250 field-emission gun scanning electron microscope (Quanta, Hillsboro, OR). ImageJ 1.43u software (National Institutes of Health, Bethesda, MD) was utilized to quantify NP size. NP surface zeta potential was quantified using a Zetasizer Nano ZS (Malvern Instruments Ltd., Malvern, UK) at 0.1 mg/mL in nanopure water.

To evaluate drug release kinetics, Mito-Met-loaded NF-NPs and CPTP-NPs (M:NF-NPs or M:CPTP-NPs, respectively) were suspended in 1x phosphate-buffered saline, pH 7.4, sonicated for 30 s, and incubated in a 37°C rotator. To maintain perfect sink conditions, phosphate-buffered saline was replaced at 0.5, 1, 2, 4, and 8 h, and at 1, 2, 3, 5 and 7 days by centrifugation, supernatant collection and resuspension in 1x phosphate-buffered saline. After 7 days, the degraded NPs were suspended in 100 m*M* sodium hydroxide to ensure complete extraction of Mito-Met. Each sample was concentrated 10× by lyophilization and resuspension in water, and the amount of drug was quantified using high-performance liquid chromatography instrument (Agilent 1200 system, Agilent, Santa Clara, CA). The poroshell 120 hydrophilic interaction liquid chromatographic column, dimensions 150 mm × 2.1 mm, 4 μm (Agilent, Santa Clara, CA) was used with a mobile phase of nanopure water + 0.1% trifluoroacetic acid (solvent A), acetonitrile (solvent B), and methanol (solvent C). A gradient from 0.1% A, 94.9% B, and 5% C at 0 min to 45% A, 50% B and 5% C at 7 min with a flow rate of 1 mL/min was used. Samples were compared to a standard curve of soluble Mito-Met in nanopure water from 2 to 200 μg/mL.

2.4 | N27 cell culture and NP safety

A rat mesencephalic neuronal cell line (N27) was used for cytotoxicity, efficacy and localization experiments.[15,48-51] Cells were thawed from liquid nitrogen and grown in RPMI media supplemented with 10% (v/v) fetal bovine serum, 2 m*M* L-glutamine, 100 U/mL penicillin, and streptomycin (10% RPMI). Upon reaching 70–90% confluence, cells were passaged by trypsinization. For 96, 24, or 6-well plates, cells were added at 5,000, 20,000 cells/well, or 80,000 cells/well in 100, 500 or 2000 μL of 10% RPMI, respectively.

To determine safe NP concentrations in N27 cells, NF-NPs and CPTP-NPs were sonicated in 2% RPMI for 30 s using a probe sonicator at 50%, diluted to 10, 30 or 100 μg/mL and added to cells at 70% confluence in a 96-well plate for 24 h. Sytox™ Green and Hoechst 33258 were diluted 1:5000 in 0% RPMI and added to each well 30 min before measuring the fluorescence on a spectrophotometer (SpectraMax 190, Molecular Devices, San Jose, CA).

2.5 | NP internalization by neuronal cells

To test cellular internalization of NPs, QD-loaded NF-NPs and CPTP-NPs (QD:NF-NPs and QD:CPTP-NPs, respectively) were added to N27 cells in a 6-well plate for 24 h. Cells were collected by trypsinization and centrifuged at 1,000 rpm for 7 min. The cells were rinsed once with ice-cold 1× phosphate-buffered saline, and then suspended in ice-cold 4% paraformaldehyde and stored at 4°C in the dark overnight. The next day, cell suspensions were added to plastic tubes and analyzed by a flow cytometer (FACSCanto, BD Biosciences, San Jose, CA) at 488 nm. Controls included cells not treated with QD:NPs and cells treated with a degraded NP control. For degraded NP control, QD:NPs were suspended in 2% RPMI at 30 μg/mL and incubated in a 37°C rotator for 24 h before adding to cells. After 24 h, released QDs were collected by centrifugating NPs and retaining supernatant. This supernatant was added to cells to confirm that fluorescence observed in QD:NP groups was due to NP internalization and not by QD release and subsequent internalization.

To confirm NP internalization in N27 cells, QD:NF-NPs or QD:CPTP-NPs were added to cells in a 24-well plate with coverslips treated with poly-D-lysine for 12 h. After 24 h, the media was aspirated and the cells were washed in prewarmed 0% Dulbecco's Modified Eagle's Medium. Next, cells were incubated with 0% Dulbecco's Modified Eagle's Medium containing 1:5,000 MitoTracker® Red and 1:10,000 Hoechst 33258 for 10 min. Cells were washed four times with pre-warmed phosphate-buffered saline and fixed with 4% paraformaldehyde. Coverslips were mounted onto SuperFrost® slides (ThermoFisher Scientific) and imaged using a confocal microscope (SP5 X MP confocal/multiphoton microscope, Leica Biosystems, Wetzlar, Germany). Controls included cells not treated with QD:NPs.

2.6 | NP efficacy against mitochondrial dysfunction

NP efficacy in protecting against rotenone-induced mitochondrial dysfunction was performed similarly to previous rotenone toxicity experiments, with some modifications.[5] Specifically, after cells reached 70% confluence and display healthy morphology, M:NF-NPs, M:CPTP-NPs or soluble Mito-Met in 2% RPMI were added to cells in a 96-well plate 24 h before reading. The administered concentration of Mito-Met in all treated groups was 30 n*M*. Negative controls included cells incubated with 2% RPMI only. All media, with or without treatment groups, was replaced with fresh 0% RPMI 7 h before reading. 6 h before reading, 1 μ*M* rotenone was added to each well, except for negative controls. Positive controls included untreated cells incubated with rotenone. Next, Sytox™ and Hoechst staining experiments were performed as previously described.[15,49,51] Specifically, Sytox™ Green

TABLE 1 NP size, morphology and surface zeta potential of all formulations

NP formulation	Encapsulated payload	Geometric diameter (nm), avg ± *SD*	Zeta potential (mV), arithmetic avg ± *SE*
NF-NP	None	310 ± 1.3	−21 ± 2
	0.2% Mito-Met	430 ± 1.4	−26 ± 0.2
	1% QD	260 ± 1.5	−26 ± 0.5
CPTP-NP	None	330 ± 1.3	4.0 ± 0.2
	0.2% Mito-Met	370 ± 1.3	−6.2 ± 0.9
	1% QD	250 ± 1.4	0.25 ± 0.3

Abbreviations: CPTP-NP, (3-carboxypropyl)triphenylphosphonium-functionalized nanoparticles; Mito-Met, triphenylphosphonium-functionalized metformin; NF-NP, nonfunctionalized nanoparticles; QD, quantum dots.

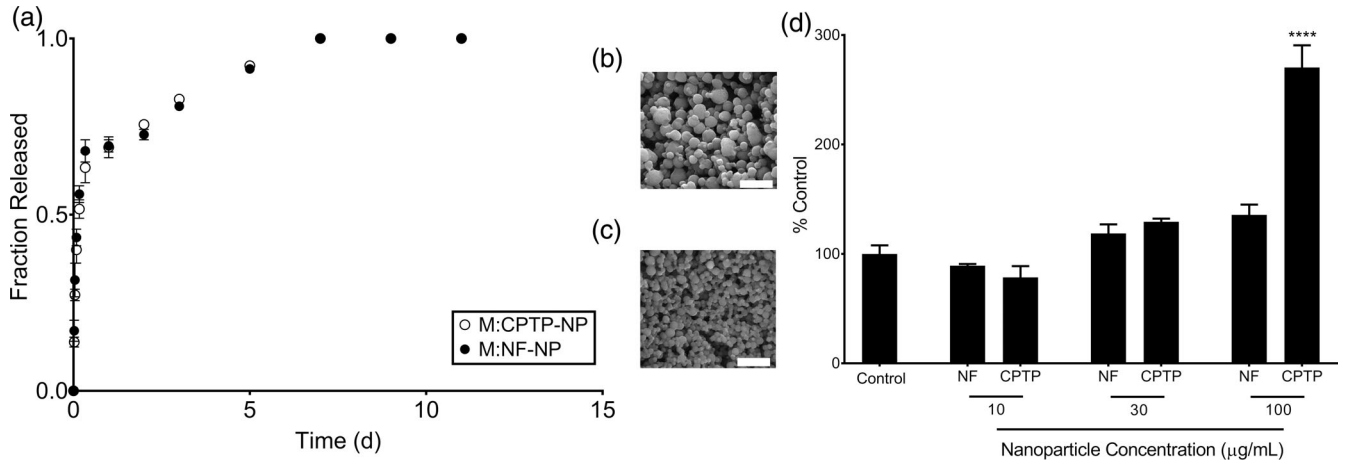

FIGURE 2 (a) Release kinetics of mito-metformin from M:CPTP-NPs and M:NF-NPs in 0.5 mL 1× PBS at 37°C, showing a large (~70%) burst release in the first few hours accompanied by sustained release for 2 weeks. The EE of M:CPTP-NPs and M:NF-NPs was 56% and 54%, respectively. $n = 3$ for M:NF-NPs and M:CPTP-NPs across one experiment. (b) and (c) Representative SEM images of NF-NPs and CPTP-NPs, respectively. Scale bars: 0.5 μm. (d) NF-NP and CPTP-NP biocompatibility in N27 cells. Cells were incubated with NPs in 2% RPMI added at 24 h, and again at 7 h before assessing cell viability using a Sytox™ Green live/dead assay. NF-NPs were found to be nontoxic at all concentrations tested, however CPTP-NPs were cytotoxic at 100 μg/mL. Control is cells in 2% RPMI only. $n = 3$ for control and for each concentration of M:NF-NPs and M:CPTP-NPs across one experiment. ****$p \leq 0.0001$ versus Control

(ex/em: 504/523 nm) and Hoechst 33258 (ex/em: 352/461 nm) were added 30 min before reading the plate and taking images.

2.7 | Statistical analysis

NP toxicity, internalization, and efficacy data were analyzed using a one-way ANOVA with multiple comparisons on GraphPad Prism® software (San Diego, CA). Comparisons were marked for significance at *p*-values less than 0.05, 0.01 and 0.001, and 0.0001. All error bars represent the standard error of the mean.

3 | RESULTS

3.1 | Characterization of functionalized copolymer

The synthesized 20:80 CPH:SA copolymer (Figure 1c) was in the appropriate molecular weight range (M_n = 13,100–21,500 Da) for synthesizing NPs, consistent with previous work.[52] After CPTP functionalization, the molecular weight of the copolymer decreased slightly (M_n = 11,700–13,000 Da), however this decrease did not significantly impact NP size and morphology (Table 1 and Figure 2b,c). Proton nuclear magnetic resonance end-group analysis of purified polymer showed functionalization with the appearance of phenyl group peaks representing CPTP (Figure 1d) and an estimated percent end-group functionalization of 45%. ATR-FTIR analysis of purified polymer confirmed functionalization with the appearance of a CH_2 bending peak that is associated with CPTP (Figure 1e).

3.2 | Nanoparticle characterization and drug release kinetics

All NF-NP and CPTP-NP formulations were spherical and discrete, ca. 300–400 nm in diameter, and well-suspended (Table 1). However, QD-encapsulated NPs resulted in slightly lower size NPs, ca. 250 nm, which may be due to the QDs providing more nucleation sites for

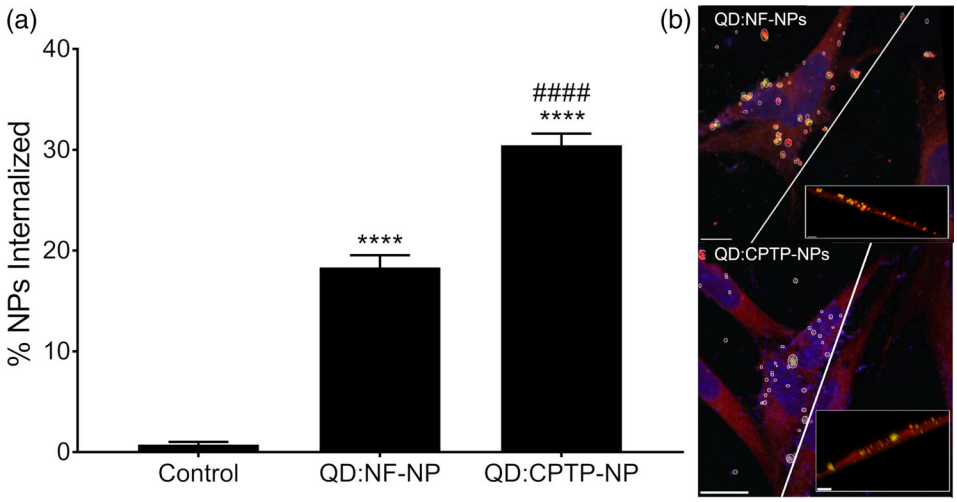

FIGURE 3 (a) QD:NP internalization in N27 cells. Cells were incubated with NPs for 24 h before fixing with 4% paraformaldehyde. Cells were sorted at 488 nm using a flow cytometer. Controls included cells treated with QDs released from NPs in 2% RPMI in a 24 h period, which were subtracted from the respective NP groups, as wells as cells in 2% RPMI only (shown). Cells incubated with QD:NF-NPs and QD:CPTP-NPs displayed significant fluorescence above background, and cells incubated with QD:CPTP-NPs displayed significantly more fluorescence than QD:NF-NPs. $n = 3$ for control, M:NF-NPs and M:CPTP-NPs across two experiments. $^{****}p \leq 0.0001$ versus control, #### $p \leq 0.0001$ versus QD:NF-NP. (b) Confocal microscopy of QD:NF-NPs or QD:CPTP-NPs incubated with N27 cells for 24 h. Cells were treated with MitoTracker® Red and Hoechst. In the image: red represents mitochondria, blue represents nuclei, and yellow-green represents NPs. White circles are drawn around NPs to show their location more clearly. Controls included cells not treated with NPs (not shown). $n = 3$ for control, QD:NF-NPs and QD:CPTP-NPs across one experiment. Scale bars: 10 μm. Inset scale bar: 5 μm

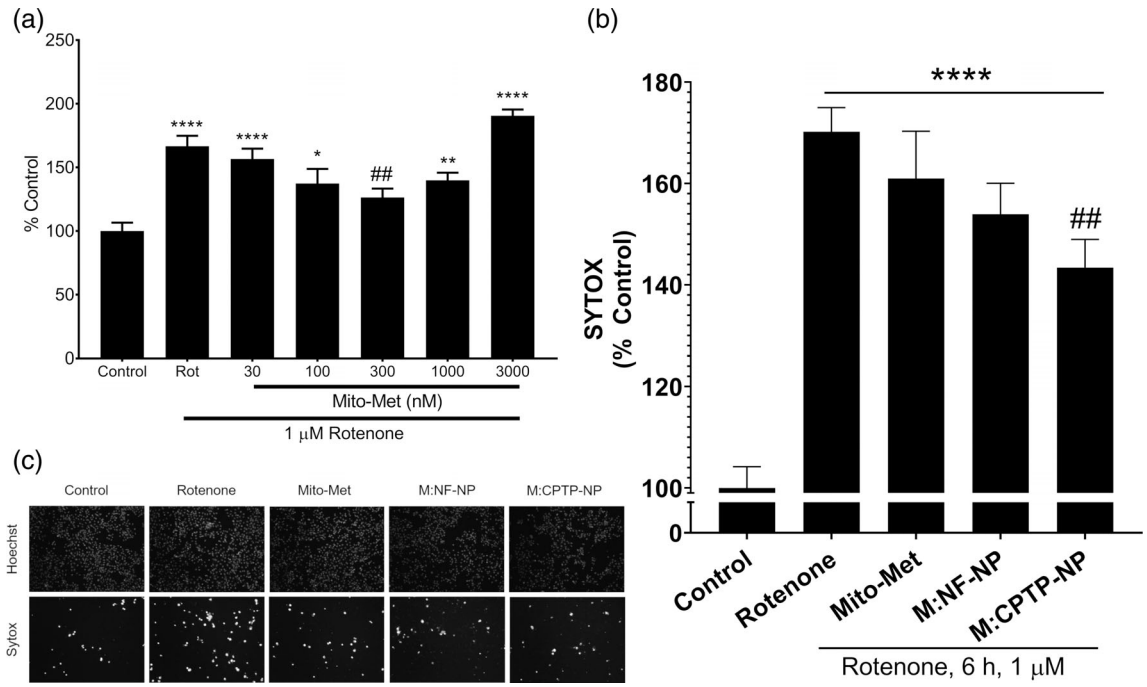

FIGURE 4 (a) Safety/efficacy study of Mito-Met. N27 cells were challenged with rotenone after being treated with Mito-Met. Controls included cells only challenged with rotenone, and cells not treated with Mito-Met. Sytox and Hoechst fluorescence was measured on a spectrophotometer. $n = 6$ across two experiments. $^{*}p \leq 0.05$, $^{**}p \leq 0.01$, $^{***}p \leq 0.001$, $^{****}p \leq 0.0001$ versus control, ## $p \leq 0.01$ versus rotenone. (b) N27 cells were challenged with rotenone after being treated with Mito-Met, M:NF-NP, or M:CPTP-NP. Controls included cells only challenged with rotenone, and cells not treated with Mito-Met, NPs or rotenone. Cell viability was assessed using a Sytox™ Green live/dead assay. Rotenone induced a significant level of toxicity above control, however M:CPTP-NP pretreatment significantly protected cells against rotenone-induced toxicity. $n = 6$ for control, M:NF-NPs and M:CPTP-NPs across three experiments. $^{****}p \leq 0.0001$ versus control, ## $p \leq 0.01$ versus rotenone. (c) representative images from efficacy study in (b)

nanoparticle formation. The NF-NP formulations were negatively charged (as measured by zeta potential) which is consistent with previous work.[26] However, CPTP functionalization of NPs led to near-zero zeta potentials (Table 1, Figure S1), consistent with the cationic nature of triphenylphosphonium.[45] Additionally, both NF-NPs and CPTP-NPs displayed similar release kinetics (Figure 2a) and encapsulation efficiency (EE) of Mito-Met, with 54% and 56% EE of the drug for M:NF-NPs and M:CPTP-NPs, respectively. Both nanoformulations showed a large burst release of Mito-Met, followed by sustained release of the drug for up to 1 week.

3.3 | NF-NPs and CPTP-NPs internalization and efficacy in N27 cells

Both NF-NPs and CPTP-NPs were well-tolerated by the cells up to NP concentrations of 30 μg/mL for 24 h (Figure 2d) as indicated by cytotoxicity studies with the Sytox™ assay. The NF-NPs did not induce any toxicity at a concentration of 100 μg/mL, while the CPTP-NPs displayed toxicity at this concentration. Based on these results, a 30 μg/mL NP concentration was used in the subsequent studies. After incubating N27 cells with 30 μg/mL QD:NF-NPs and QD:CPTP-NPs for 24 h, it was found that QD:CPTP-NPs are internalized by a significantly larger percent of N27 cells than QD:NF-NPs, with 31% and 18% of cells internalizing QD:CPTP-NPs and QD:NF-NPs, respectively (Figure 3a). Confocal microscopy experiments confirmed these results and determined that the NPs are internalized, and not just associating with the cell membrane (Figure 3b).

A Mito-Met safety and efficacy study was performed in N27 cells to identify the optimal concentration of soluble drug in this assay (Figure 4a). It was observed that Mito-Met concentrations above 300 n*M* appear to be increasingly toxic to neuronal cells. Additionally, Mito-Met concentrations below 300 n*M* Mito-Met were observed to be ineffective in protecting against rotenone (Figure 4a). However, after treating N27 cells with M:NF-NPs, M:CPTP-NPs or soluble Mito-Met followed by challenging with rotenone, only M:CPTP-NPs protected cells against rotenone-induced mitochondrial dysfunction (Figure 4b,c). Notably, the concentration of Mito-Met in these formulations was 30 n*M*, an order of magnitude less than the effective soluble dose of Mito-Met.

4 | DISCUSSION

Mitochondrial dysfunction is a signature mechanism that contributes to the progression of neurodegenerative disease.[26] Mitochondrial dysfunction induces oxidative stress in the brain through the formation of reactive oxygen species and reactive nitrogen species.[26,53] Specifically, a deficiency in complex I of the mitochondrial transport chain plays a key role in mitochondrial dysfunction and ensuing processes in PD.[5,53] Therefore, the discovery and optimization of mitochondrial-targeted therapeutics could significantly improve PD treatment.

Rotenone-based challenge models, both in vitro and in vivo, of PD are used due to the ability to recapitulate primary pathological mechanisms like mitochondrial dysfunction and subsequent oxidative stress of dopaminergic neurons.[4-6] For example, a rotenone toxicology model has been used to induce mitochondrial dysfunction N27 cells.[5] In previous work, Mito-Met has shown neuroprotective capabilities in protecting cells from rotenone-induced mitochondrial dysfunction by AMPK activation and other associated neuroprotective mechanisms at a much lower dose compared to metformin alone.[12] However, while lower, therapeutic doses are neuroprotective, higher doses can become cytotoxic (Figure 4a), and so minimizing therapeutic dose would be beneficial for slow down neurodegeneration. By providing both sustained and targeted release, CPTP-functionalized polyanhydride NPs could alleviate this issue and further optimize treatment regimen.

A recent review elucidates the importance of nano-carrier targeting strategies for neurodegenerative applications.[18] The need to overcome multiscale hurdles to brain delivery for PD, including crossing the BBB, reaching dopaminergic neurons, and in many cases, targeting the mitochondria, makes optimization of targeting strategies challenging.[18] The selection of the right targeting ligand, or set of targeting ligands, if applicable, such that it improves targeting at all three scales is critical for optimizing a NP platform-based treatment regimen.[18] The targeting ligand TPP has improved both brain localization and mitochondrial targeting for different types of NPs.[44,46,47,54-57] However, the ability of TPP-based ligands such as CPTP to improve targeting and cellular internalization of NPs in dopaminergic neurons has not yet been investigated.

SA-rich polyanhydride chemistries, due to their lipophilic nature, show higher levels of cellular internalization compared to other polyanhydride chemistries.[40] The 20:80 CPH:SA NP chemistry used in this study has been surface functionalized with targeting ligands to further improve targeting and cellular internalization,[26] and has also shown high levels of cellular internalization in an in vitro BBB model.[41] However, the combination of polyanhydride NP surface erosion as well as the extended length of time that NPs would be exposed to aqueous degradation conditions before reaching neurons in vivo present limitations for NP surface functionalization methods.

To address this limitation, a unique functionalization method was developed in this work that enabled a longer persistence time for the targeting ligand on polyanhydride NPs. Specifically, CPTP was conjugated to 20:80 CPH:SA copolymer by an anhydride interchange mechanism, which is the same mechanism used to polymerize polyanhydrides. By tuning the reaction conditions, further polymerization did not take place and instead the polymer was functionalized with CPTP. Confirmation of successful functionalization using this technique was verified by ^{1}H nuclear magnetic resonance, with the existence of CPTP phenyl group peaks (Figure 1d), and by Fourier transform infrared spectroscopy—attenuated total reflectance, with the presence of CPTP CH_2 bending peaks (Figure 1e) in the polymer.

An additional limitation of surface-functionalizing polyanhydride NPs using techniques such as carbodiimide crosslinking chemistry is that the polyanhydride NPs surfaces erode and may prematurely

release encapsulated payloads during the functionalization. In contrast, bulk functionalization of the polymer eliminates this shortcoming because the NPs are not exposed to degradation conditions before treatment. Consistent with this argument, drug release kinetics profiles from both functionalized and nonfunctionalized NPs were unchanged (Figure 2a), as were their EEs (54% and 56% for NF-NPs and CPTP-NPs, respectively).

It is possible that increased cytotoxicity seen with triphenylphosphonium-conjugated compounds may be associated with the cationic nature of triphenylphosphonium.[45] Therefore, it was necessary to determine a safely tolerated concentration of NF-NPs and CPTP-NPs in N27 cells. At an NP concentration of 30 μg/mL, neither NF-NPs nor CPTP-NPs were cytotoxic, on the other hand CPTP-NPs at 100 μg/mL were cytotoxic, indicating that CPTP functionalization did not impact CPTP-NP biocompatibility up to 30 μg/mL (Figure 2d). Therefore, this NP concentration was used for subsequent studies with both formulations.

The high levels of neuronal internalization observed with compounds conjugated to TPP and its derivatives are related to its cationic and lipophilic properties.[42-47] Therefore, conjugating CPTP to 20:80 CPH:SA copolymer may further improve targeting and therefore cellular internalization of therapeutic-encapsulated NPs. After incubating the QD:NPs with N27 cells, it was found that QD:CPTP-NPs were internalized by significantly more cells than QD:NF-NPs (Figure 3a). Importantly, CPTP-NPs showed significantly less negative surface zeta potentials, and in some cases even positive zeta potentials. The cationic nature of CPTP is a likely cause for this shift in zeta potential across all formulations.[45] The correlation with higher CPTP-NP internalization by N27 cells suggests that CPTP-NPs have a stronger nonspecific interaction with the negatively charged cell membrane, which may explain the higher cellular internalization efficiency.[55]

After showing that CPTP significantly enhanced cellular internalization of this NP formulation, the ability of this formulation to translate into better protection of Mito-Met against environmental toxins was tested. Rotenone is a widely used pesticide that is toxic to dopaminergic neurons.[4] The neuroprotective drug Mito-Met acts to reduce the extent of mitochondrial dysfunction associated with rotenone exposure to cells through AMPK activation and subsequent restoration of neuronal energy balance.[14] Low dose Mito-Met (300 n*M*) has been shown to protect against rotenone-induced mitochondrial dysfunction in a dopaminergic cell line.[12] However, at higher concentrations, Mito-Met can be cytotoxic to the targeted cells (see Figure 4a) by inhibiting complex I of the electron transport chain, which while beneficial for cancer treatment,[58] is detrimental when treating neuronal cells against rotenone-induced toxicity. Therefore, minimizing the effective therapeutic dose of Mito-Met could be beneficial for anti-neurodegenerative applications.

In this study, a 30 n*M* soluble Mito-Met dose, which is an order of magnitude lower than the previously reported optimal dose for treatment of rotenone-induced mitochondrial dysfunction in N27 cells, did not protect against rotenone, as shown in Figure 4. Cells treated with M:NF-NPs containing 30 n*M* Mito-Met lowered rotenone-induced toxicity but did not significantly reduce cell death (Figure 4b). However, the use of M:CPTP-NPs containing 30 n*M* Mito-Met led to significantly better protection against rotenone challenge (Figure 4b). Due to the potentially cytotoxic nature of cationic molecules like Mito-Met at high concentrations, the dose-sparing and sustained release of Mito-Met provided by the functionalized polyanhydride NPs can minimize systemic toxicity while still protecting against mitochondrial dysfunction.

Considering the significance of mitochondrial dysfunction in PD, the optimization of treatment regimen to deliver mitochondrial-targeted drugs such as Mito-Met could lead to more effective therapies for PD. The success of the mitochondria-targeted nanomedicine treatment regimen in ameliorating rotenone-induced damage discussed in this work warrants further investigation into the mechanism by which the CPTP-NPs improve mitochondrial function, both in vitro and in vivo.

5 | CONCLUSIONS

There is a need to discover therapeutics that treat the underlying mechanisms to PD. Of these, mitochondrial dysfunction plays a major role in contributing to the death of dopaminergic cells. Due to the low cellular internalization efficiency of approved anti-neurodegenerative therapeutics, effective doses are often too high and too frequent, resulting in systemic toxicity. Drug-encapsulated targeted polyanhydride NPs can minimize the dose by improving targeting efficiency to mitochondria and providing sustained release of therapeutics. In this work, enhanced cellular internalization of a targeted polyanhydride NP formulation, CPTP-NPs, was correlated with protection of N27 cells against rotenone-induced cytotoxicity with significant dose-sparing of the drug Mito-Met. The demonstrated success in using the novel polyanhydride NP functionalization method to improve therapeutic efficacy in vitro lays the foundation for the development of nanomedicine therapies for PD and other neurodegenerative conditions.

ACKNOWLEDGMENTS

The authors would like to acknowledge funding support from the US Army Medical Research and Materiel Command under contract W81XWH-11-1-0700. The authors are additionally grateful to the Iowa State Nanovaccine Institute.

AUTHOR CONTRIBUTIONS

BWS performed cell culture, release study and polymer/nanoparticle synthesis and characterization experiments. BWS performed all the experimental analysis. RLS and MGP synthesized QDs for use in N27 internalization experiments. BWS, VA, BN, and SKM performed experimental design, including formulations and controls. BK synthesized Mito-Apo and Mito-Met for use in cell culture and release study experiments. BWS wrote the manuscript. AGK, VA, BN, and SKM edited the manuscript. All authors have given approval to the final version of the manuscript.

DISCLOSURE

Balaji Narasimhan is a co-founder of ImmunoNanoMed Inc., a start-up in Ames, IA with business interests in the development of nano-based vaccines against infectious diseases. He also has a financial interest in Degimflex LLC (see below). Surya Mallapragada is a co-founder of Degimflex LLC., a start-up in Ames, IA with business interests in the development of flexible degradable electronic films for biomedical applications. She also has a financial interest in ImmunoNanoMed Inc. Anumantha Kanthasamy and Vellareddy Anantharam have an equity interest in PK Biosciences Corporation located in Ames, IA. Anumantha Kanthasamy also has an equity interest in Probiome Therapeutics located in Ames, IA. The terms of this arrangement have been reviewed and approved by Iowa State University in accordance with its conflict of interest policies. Other authors declare no actual or potential competing financial interests.

DATA AVAILABILITY STATEMENT

The data that support the findings of this study are available from the corresponding author upon reasonable request.

REFERENCES

1. Statistics on Parkinson's Disease Parkinson association of the Carolinas; 2013. https://www.parkinsonassociation.org/facts-about-parkinsons-disease/. Accessed Jul 23, 2021.
2. Environmental Factors Parkinson's Foundation; 2018. http://parkinson.org/Understanding-Parkinsons/Causes-and-Statistics/Environmental-Factors. Accessed Jul 23, 2021.
3. Dauer W, Przedborski S. Parkinson's disease: mechanisms and models. *Neuron*. 2003;*39*(6):889-909.
4. De Boel L, Sarah C. Mechanism of toxicity in rotenone models of Parkinson's disease. *J Neurosci*. 2015;*23*(34):10756-10764.
5. Charli A, Jin H, Anantharam V, Kanthasamy A, Kanthasamy AG. Alterations in mitochondrial dynamics induced by tebufenpyrad and pyridaben in a dopaminergic neuronal cell culture model. *Neurotoxicology*. 2016;*53*:302-313.
6. Pan-Montojo F, Anichtchik O, Dening Y, et al. Progression of Parkinson's disease pathology is reproduced by intragastric administration of rotenone in mice. *PLoS ONE*. 2010;*5*(1):e8762. https://doi.org/10.1371/journal.pone.0008762
7. Gordon R, Singh N, Lawana V, et al. Protein kinase Cδ upregulation in microglia drives neuroinflammatory responses and dopaminergic neurodegeneration in experimental models of Parkinson's disease. *Neurobiol Dis*. 2016;*93*:96-114.
8. Heathcote HR, Mancini SJ, Strembitska A, et al. Protein kinase C phosphorylates AMP-activated protein kinase α1 Ser487. *Biochem J*. 2016;*473*(24):4681-4697.
9. Choi JS, Park C, Jeong JW. AMP-activated protein kinase is activated in Parkinson's disease models mediated by 1-methyl-4-phenyl-1,-2,3,6-tetrahydropyridine. *Biochem Biophys Res Commun*. 2010;*391*(1):147-151. https://doi.org/10.1016/j.bbrc.2009.11.022
10. Porceddu PF, Ishola IO, Contu L, Morelli M. Metformin prevented dopaminergic neurotoxicity induced by 3,4-methylenedioxymethamphetamine administration. *Neurotox Res*. 2016;*30*(1):101-109. https://doi.org/10.1007/s12640-016-9633-5
11. Cheng G, Zielonka J, Ouari O, et al. Mitochondria-targeted analogues of metformin exhibit enhanced antiproliferative and radiosensitizing effects in pancreatic cancer cells. *Cancer Res*. 2016;*76*(13):3904-3915. https://doi.org/10.1158/0008-5472.CAN-15-2534
12. Kanthasamy A, Kalyanaraman B. *Neuroprotection by mitochondria-targeted metformin*. 2020. (US patent US10576093B2). United States Patent and Trademark Office. https://patents.google.com/patent/US10576093B2/en,
13. Galluzzi L. Pharmacological modulation of autophagy: therapeutic potential and persisting obstacles. *Nat Rev Drug Discov*. 2017;*16*(7):487-511. https://doi.org/10.1038/nrd.2017.22
14. Ronnett GV, Ramamurthy S, Kleman AM, Landree LE, Aja S. AMPK in the brain: its roles in energy balance and neuroprotection. *J Neurochem*. 2009;*109*(Suppl 1):17-23.
15. Langley M, Ghosh A, Charli A, et al. Mito-apocynin prevents mitochondrial dysfunction, microglial activation, oxidative damage and progressive neurodegeneration in MitoPark transgenic mice. *Antioxid Redox Signal*. 2017;*27*(14):1048-1066.
16. Ghosh A, Langley MR, Harischandra DS, et al. Mitoapocynin treatment protects against neuroinflammation and dopaminergic neurodegeneration in a preclinical animal model of Parkinson's disease. *J Neuroimmune Pharmacol*. 2016;*11*(2):259-278.
17. Ross KA, Brenza TM, Binnebose AM, et al. Nano-enabled delivery of diverse payloads across complex biological barriers. *J Controlled Release: Off J Controll Release Soc*. 2015;*219*:548-559.
18. Mullis AS, Schlichtmann BW, Narasimhan B, Cademartiri R, Mallapragada SK. Ligand-cascading nano-delivery devices to enable multiscale targeting of anti-neurodegenerative therapeutics. *Biomed Mater*. 2018;*13*(3):034102.
19. Bhattamisra SK, Shak AT, Xi LW, et al. Nose to brain delivery of rotigotine loaded chitosan nanoparticles in human SH-SY5Y neuroblastoma cells and animal model of Parkinson's disease. *Int J Pharm*. 2020;*579*(119148). https://doi.org/10.1016/j.ijpharm.2020.119148.
20. Park ES, Maniar M, Shah JC. Biodegradable polyanhydride devices of cefazolin sodium, bupivacaine, and taxol for local drug delivery: preparation, and kinetics and mechanism of in vitro release. *J Control Release*. 1998;*52*(1–2):179-189.
21. Storm PB, Moriarity JL, Tyler B, Burger PC, Brem H, Weingart J. Polymer delivery of camptothecin against 9L gliosarcoma: release, distribution, and efficacy. *J Neurooncol*. 2002;*56*(3):209-217.
22. Masters DB, Berde CB, Dutta S, Turek T, Langer R. Sustained local anesthetic release from bioerodible polymer matrices: a potential method for prolonged regional anesthesia. *Pharm Res: Off J Am Assoc Pharm Sci*. 1993;*10*(10):1527-1532.
23. Carrillo-Conde BR, Darling RJ, Seiler SJ, Ramer-Tait AE, Wannemuehler MJ, Narasimhan B. Sustained release and stabilization of therapeutic antibodies using amphiphilic polyanhydride nanoparticles. *Chem Eng Sci*. 2015;*125*:98-107.
24. Torres MP, Determan AS, Anderson GL, Mallapragada SK, Narasimhan B. Amphiphilic polyanhydrides for protein stabilization and release. *Biomaterials*. 2007;*28*(1):108-116.
25. Determan AS, Trewyn BG, Lin VSY, Nilsen-Hamilton M, Narasimhan B. Encapsulation, stabilization, and release of BSA-FITC from polyanhydride microspheres. *J Control Release*. 2004;*100*(1):97-109.
26. Brenza TM, Ghaisas S, Ramirez JVJEV, et al. Neuronal protection against oxidative insult by polyanhydride nanoparticle-based mitochondria-targeted antioxidant therapy. *Nanomed Nanotechnol Biol Med*. 2017;*13*(3):809-820.
27. Tabata Y, Langer R. Polyanhydride Mierospheres that display near-constant release of water-soluble model drug compounds. *Pharm Res: Off J Am Assoc Pharm Sci*. 1993;*10*(3):391-399.
28. Kumar N, Langer RS, Domb AJ. Polyanhydrides: an overview. *Adv Drug Deliv Rev*. 2002;*54*(7):889-910.
29. Katti DS, Lakshmi S, Langer R, Laurencin CT. Toxicity, biodegradation and elimination of polyanhydrides. *Adv Drug Deliv Rev*. 2002;*54*(7):933-961.
30. Jain JP, Modi S, Kumar N. Hydroxy fatty acid based polyanhydride as drug delivery system: synthesis, characterization, in vitro degradation, drug release, and biocompatibility. *J Biomed Mater Res*. 2008;*84*(3):740-752.
31. Vela-Ramirez JE, Goodman JT, Boggiatto PM, et al. Safety and biocompatibility of carbohydrate-functionalized polyanhydride nanoparticles. *AAPS J*. 2015;*17*(1):256-267.

32. Westphal M, Ram Z, Riddle V, Hilt D, Bortey E. Gliadel® wafer in initial surgery for malignant glioma: long-term follow-up of a multicenter controlled trial. *Acta Neurochir*. 2006;*148*(3):269-275.
33. Göpferich A, Tessmar J. Polyanhydride degradation and erosion. *Adv Drug Deliv Rev*. 2002;*54*(7):911-931.
34. Shieh L, Tamada J, Chen I, Pang J, Domb A, Langer R. Erosion of a new family of biodegradable polyanhydrides. *J Biomed Mater Res*. 1994;*28*(12):1465-1475.
35. Larobina D, Mensitieri G, Kipper MJ, Narasimhan B. Mechanistic understanding of degradation in bioerodible polymers for drug delivery. *AIChE J*. 2002;*48*(12):2960-2970.
36. Ulery BD, Kan HM, Williams BA, et al. Facile fabrication of polyanhydride/anesthetic nanoparticles with tunable release kinetics. *Adv Healthc Mater*. 2014;*3*(6):843-847.
37. Petersen LK, Determan AS, Westgate C, Bendickson L, Nilsen-Hamilton M, Narasimhan B. Lipocalin-2-loaded amphiphilic polyanhydride microparticles accelerate cell migration. Journal of biomaterials science. *Polym Ed*. 2011;*22*(9):1237-1252.
38. Binnebose AM, Haughney SL, Martin R, Imerman PM, Narasimhan B, Bellaire BH. Polyanhydride nanoparticle delivery platform dramatically enhances killing of filarial worms. *PLoS Negl Trop Dis*. 2015;*9*(10):e0004173.
39. Huntimer L, Wilson Welder JH, Ross K, et al. Single immunization with a suboptimal antigen dose encapsulated into polyanhydride microparticles promotes high titer and avid antibody responses. *J Biomed Mater Res—Pt B Appl Biomater*. 2013;*101B*:91-98.
40. Phanse Y, Lueth P, Ramer-Tait AE, et al. Cellular internalization mechanisms of polyanhydride particles: implications for rational design of drug delivery vehicles. *J Biomed Nanotechnol*. 2016;*12*(7):1544-1552.
41. Brenza TM, Schlichtmann BW, Bhargavan B, et al. Biodegradable polyanhydride-based nanomedicines for blood to brain drug delivery. *J Biomed Mater Res Pt A*. 2018;*106*(11):2881-2890.
42. Murphy MP, Smith RAJ. Targeting antioxidants to mitochondria by conjugation to lipophilic cations. *Drug-Induced Mitochondr Dysfunct*. 2007;*47*:629-656.
43. Lei W, Xie J, Hou Y, et al. Mitochondria-targeting properties and photodynamic activities of porphyrin derivatives bearing cationic pendant. *J Photochem Photobiol B Biol*. 2010;*98*(2):167-171.
44. Madak JT, Neamati N. Membrane permeable lipophilic cations as mitochondrial directing groups. *Curr Top Med Chem*. 2015;*15*:745-766.
45. Bielski ER, Zhong Q, Brown M, Da Rocha SRP. Effect of the conjugation density of triphenylphosphonium cation on the mitochondrial targeting of poly(amidoamine) dendrimers. *Mol Pharm*. 2015;*12*:3043-3053.
46. Marrache S, Dhar S. Engineering of blended nanoparticle platform for delivery of mitochondria-acting therapeutics. *Proc Natl Acad Sci U S A*. 2012;*109*(40):16288-16293.
47. Dhar S, Baker EW, Marrache S, West FD, Wyatt E, Marrache S, West FD. Therapeutic nanoparticles for accumulation in the brain. US Patent No. 20170216219. 2017.
48. Zhong X, Luo J, Rastogi P, Kanthasamy AG, Jiles DC. Transcranial magnetic stimulation promotes the proliferation of dopaminergic neuronal cells in vitro. *AIP Adv*. 2018;*8*(5):056709.
49. Song C, Charli A, Luo J, et al. Mechanistic interplay between autophagy and apoptotic signaling in endosulfan-induced dopaminergic neurotoxicity: relevance to the adverse outcome pathway in pesticide neurotoxicity. *Toxicol Sci*. 2019;*169*(2):333-352.
50. Xu Q, Kanthasamy AG, Reddy MB. Epigallocatechin gallate protects against TNFα- or H_2O_2-induced apoptosis by modulating iron related proteins in a cell culture model. *Int J Vitam Nutr Res*. 2018;*88*(3–4):158-165.
51. Singh N, Lawana V, Luo J, et al. Organophosphate pesticide chlorpyrifos impairs STAT1 signaling to induce dopaminergic neurotoxicity: implications for mitochondria mediated oxidative stress signaling events. *Neurobiol Dis*. 2018;*117*:82-113.
52. Ulery BD, Phanse Y, Sinha A, Wannemuehler MJ, Narasimhan B, Bellaire BH. Polymer chemistry influences monocytic uptake of polyanhydride nanospheres. *Pharm Res*. 2009;*26*(3):683-690.
53. Lin MT, Beal MF. Mitochondrial dysfunction and oxidative stress in neurodegenerative diseases. *Nature*. 2006;*443*(7113):787-795. https://doi.org/10.1038/nature05292
54. Biswas S, Dodwadkar NS, Piroyan A, Torchilin VP. Surface conjugation of triphenylphosphonium to target poly(amidoamine) dendrimers to mitochondria. *Biomaterials*. 2012;*33*:4773-4782.
55. Wang X-H, Peng H-S, Yang L, et al. Poly-l-lysine assisted synthesis of core–shell nanoparticles and conjugation with triphenylphosphonium to target mitochondria. *J Mater Chem B*. 2013;*1*:5143-5152.
56. Theodossiou TA, Sideratou Z, Katsarou ME, Tsiourvas D. Mitochondrial delivery of doxorubicin by triphenylphosphonium- functionalized hyperbranched nanocarriers results in rapid and severe cytotoxicity. *Pharm Res*. 2013;*30*(11):2832-2842.
57. Paleos CM, Tsiourvas D, Sideratou Z. Triphenylphosphonium decorated liposomes and dendritic polymers: prospective second generation drug delivery systems for targeting mitochondria. *Mol Pharm*. 2016;*13*(7):2233-2241.
58. Kalyanaraman B, Cheng G, Hardy M, et al. Modified metformin as a more potent anticancer drug: mitochondrial inhibition, redox signaling, Antiproliferative effects and future EPR studies. *Cell Biochem Biophys*. 2017;*75*(3–4):311-317. https://doi.org/10.1007/s12013-017-0796-3

SUPPORTING INFORMATION

Additional supporting information may be found online in the Supporting Information section at the end of this article.

How to cite this article: Schlichtmann, B. W., Kalyanaraman, B., Schlichtmann, R. L., Panthani, M. G., Anantharam, V., Kanthasamy, A. G., Mallapragada, S. K., & Narasimhan, B. (2022). Functionalized polyanhydride nanoparticles for improved treatment of mitochondrial dysfunction. *Journal of Biomedical Materials Research Part B: Applied Biomaterials*, *110* (2), 450–459. https://doi.org/10.1002/jbm.b.34922